

## Supporting Information

### **Anchoring Strategy Leads to Enhanced Proton Conductivity in a New Metal-Organic Framework**

Tien H. N. Lo,<sup>§[a]</sup> My V. Nguyen<sup>§[a,c]</sup> and Thach N. Tu<sup>\*[a,b]</sup>

<sup>a</sup>Center for Innovative Materials and Architectures (INOMAR), Vietnam National University-Ho Chi Minh (VNU-HCM), Ho Chi Minh City 721337, Vietnam.

<sup>b</sup>Bach Khoa University, VNU-HCM, Ho Chi Minh City 721337, Vietnam.

<sup>c</sup>University of Science, VNU-HCM, Ho Chi Minh City 721337, Vietnam.

<sup>§</sup>These author contributed equally

\*To whom correspondence should be addressed: [tnthach@inomar.edu.vn](mailto:tnthach@inomar.edu.vn)

---

## Table of Contents

---

<b>Section S1</b>	<i>Materials and Analytical Techniques</i>	<b>S3</b>
<b>Section S2</b>	<i><sup>1</sup>H-NMR Analysis for H<sub>3</sub>SNDC</i>	<b>S4</b>
<b>Section S3</b>	<i>Microscope Picture of VNU-17</i>	<b>S5</b>
<b>Section S4</b>	<i>Single Crystal X-ray Diffraction Analysis</i>	<b>S6</b>
<b>Section S5</b>	<i>Powder X-ray Diffraction Patterns</i>	<b>S7-S8</b>
<b>Section S6</b>	<i>Fourier Transform Infrared Analysis (FT-IR)</i>	<b>S9</b>
<b>Section S7</b>	<i>Thermal Gravimetric Analyses (TGA)</i>	<b>S10</b>
<b>Section S8</b>	<i>N<sub>2</sub> Adsorption Isotherm of VNU-17</i>	<b>S11</b>
<b>Section S9</b>	<i>Stability of VNU-17 in Water</i>	<b>S12-S13</b>
<b>Section S10</b>	<i><sup>1</sup>H-NMR Analysis of Digested Samples</i>	<b>S14-S15</b>
<b>Section S11</b>	<i>Rietveld Refinement of Hlm<sub>11</sub>⊂VNU-17</i>	<b>S16</b>
<b>Section S12</b>	<i>Water Adsorption Studies</i>	<b>S17-S19</b>
<b>Section S13</b>	<i>Proton Conductivity Studies</i>	<b>S20-S33</b>
<b>Section S14</b>	<i>Stability of Hlm<sub>11</sub>⊂VNU-17 during Proton Conductivity Studies</i>	<b>S34-S35</b>

---

## Section S1. Materials and Analytical Techniques

**Starting Materials and General Procedures.** 2,6- naphthalenedicarboxylic acid (H<sub>2</sub>NDC, 95%), zirconium chloride octahydrate (ZrOCl<sub>2</sub>·8H<sub>2</sub>O, 98%), imidazole (HIm, 99%), *N,N*-dimethylformamide (DMF, 99% extra dry grade), sulfuric acid (H<sub>2</sub>SO<sub>4</sub>, 98%), hydrochloric acid (HCl, 37%) and formic acid (HCOOH, 95%) were purchased from Aldrich Chemical Co. Anhydrous methanol (MeOH, 99%) and dichloromethane (CH<sub>2</sub>Cl<sub>2</sub>, 99%) were obtained from Acros Organics. All other chemicals were purchased from local vendors and all chemicals were used without further purification.

Thermal gravimetric analyses (TGA) were performed on a TA Q500 thermal analysis system under air flow. Fourier transform infrared spectroscopy (FT-IR) measurements were carried out using a Bruker Vertex 70 spectrometer with the Attenuated Total Reflectance (ATR) sampling method employed. Solution <sup>1</sup>H nuclear magnetic resonance (NMR) spectra were acquired on a Bruker Advance II-500 MHz NMR spectrometer, typically, VNU-17 (10 mg) was digested in 500 μL of DMSO-d<sub>6</sub> solution of HF (10 μL). The mixture was then sonicated for 10 minutes before <sup>1</sup>H-NMR measurement. Water uptake measurements for VNU-17, HIm<sub>9</sub>⊂VNU-17, and HIm<sub>11</sub>⊂VNU-17 were carried out using a BELSORP-aqua3 with the experiment temperature being controlled via water circulator. Elemental analyses were performed using a LECO CHNS-932 analyzer. Impedance analysis for pelletized samples of VNU-17, HIm<sub>9</sub>⊂VNU-17, and HIm<sub>11</sub>⊂VNU-17 (13 mm diameter, pressed at 3.76 ton cm<sup>-2</sup>) were carried out on a Gamry potentiostat (model: Interface 1000) using the two-probe method. Humidity was controlled by an Espec humidity chamber (model SH-222). The measuring frequency ranged from 1 MHz to 10 Hz. The applied voltage varied from 1 mV to 80 mV depending on open circle voltage. The thickness of the pellet was measured using a Nikon SMZ1000 microscope, with a typical pellet thickness ranging from 0.4 to 0.5 mm.

**Single Crystal and Powder X-ray Diffraction Analysis.** Single crystal data for VNU-17 were collected on a Bruker D8 Venture diffractometer using monochromatic fine focus Cu K<sub>α</sub> radiation (λ = 1.54178 Å), with operational conditions of 50 kW and 1.0 mA. The diffraction data was collected by a PHOTON-100 CMOS detector and the unit cell information was determined using Bruker SMART APEX II software suite. The data set was

reduced and data correction was carried out by a multi-scan spherical absorption method. The structure was solved by direct methods and further refinement was performed using the full-matrix least-squares method in the SHELX-97 program package. After locating the framework backbone atoms, the SQUEEZE routine in PLATON was used to remove residual electron density from solvent molecules located within the pores of VNU-17. The final structure was anisotropically refined using a modified electron density map obtained from the SQUEEZE routine. The crystallographic information file (CIF) of VNU-17 can be obtained, free of charge, via the Cambridge Structural Database (CCDC number: 1540864). Powder X-ray data presented herein were collected using a Bruker D8 Advance employing Ni filtered Cu K $\alpha$  ( $\lambda = 1.54178 \text{ \AA}$ ). The system was equipped with an anti-scattering shield that prevents incident diffuse radiation from hitting the detector.

## Section S2. $^1\text{H-NMR}$ analysis for $\text{H}_3\text{SNDC}$

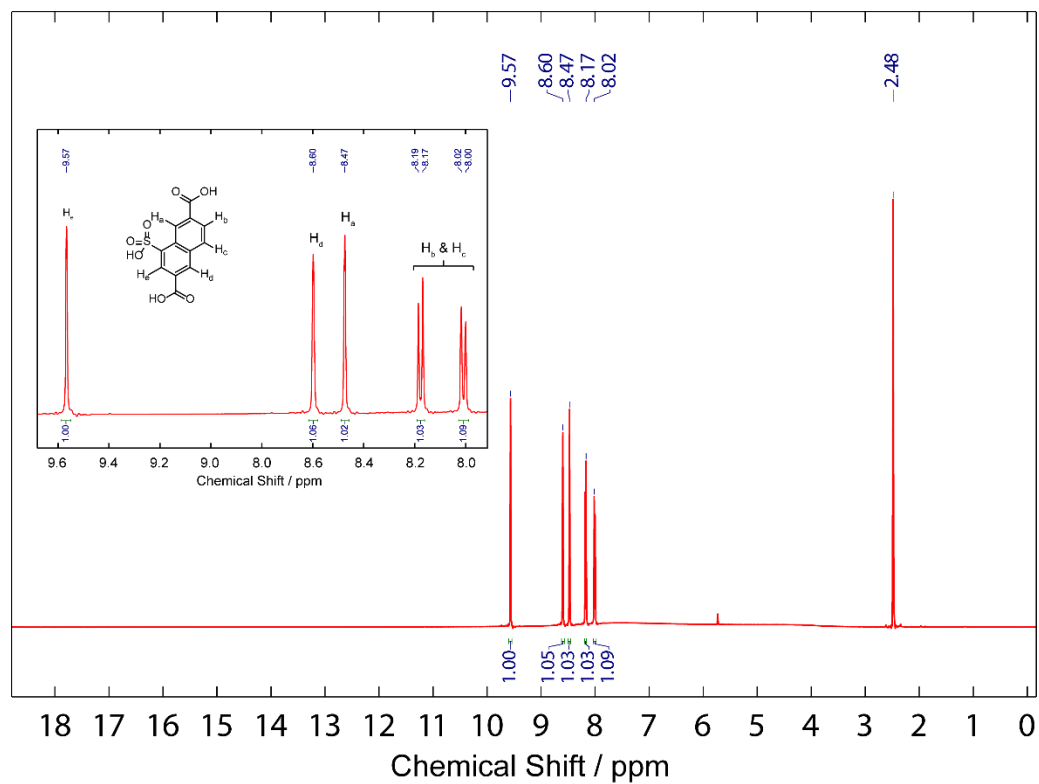


**Figure S1.**  $^1\text{H-NMR}$  analysis of the  $\text{H}_3\text{SNDC}$  linker.

**Section S3.** Microscope Picture of VNU-17

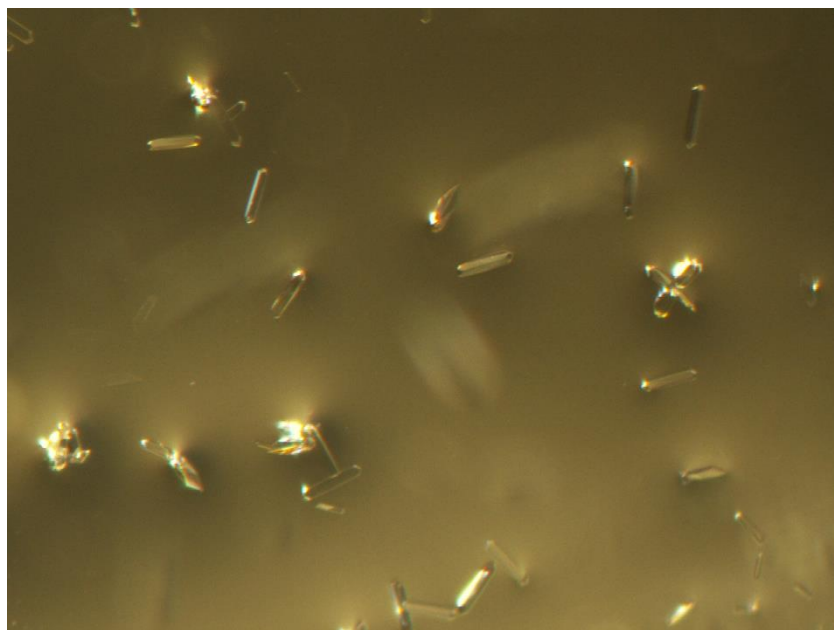


**Figure S2.** Optical microscopy picture of VNU-17 crystals.

## Section S4 Single Crystal X-ray Diffraction Analysis

**Table S1.** Crystal data and structure refinement for VNU-17

Empirical formula	C <sub>24</sub> H <sub>8</sub> O <sub>22.12</sub> S <sub>2</sub> Zr <sub>3</sub>
Formula weight	988
Temperature (K)	93
Wavelength (Å)	1.54178
Crystal system	Tetragonal
Space group	<i>I4/m</i>
Unit cell dimensions (Å)	<i>a</i> = 17.7506(5) <i>b</i> = 17.7506(5) <i>c</i> = 22.4863(7)
Volume (Å <sup>3</sup> )	7085.1(5)
Z	4
Density (g cm <sup>-3</sup> )	0.926
Absorption coefficient (mm <sup>-1</sup> )	4.501
<i>F</i> (000)	1924
Crystal size (mm)	0.068 × 0.070 × 0.173
$\theta$ range (°)	3.1463 to 65.2399.
Index ranges	-12 ≤ <i>h</i> ≤ 20, -17 ≤ <i>k</i> ≤ 20, -25 ≤ <i>l</i> ≤ 25
Reflections collected	14660
Independent reflections	2910 [ <i>R</i> <sub>int</sub> = 0.3155]
Completeness to $\theta = 62.348^\circ$	1.000
Data / restraints / parameters	14660 / 3 / 132
S (GOF)	1.060
<i>R</i> <sub>1</sub> , <i>wR</i> <sub>2</sub> [ <i>I</i> > 2 $\sigma$ ( <i>I</i> )]	0.1196, 0.2832
<i>R</i> <sub>1</sub> , <i>wR</i> <sub>2</sub> (all data)	0.1583, 0.3062
Largest diff. peak and hole (e <sup>-</sup> ·Å <sup>-3</sup> )	1.574 and -3.316

## Section S5. Powder X-ray Diffraction Patterns

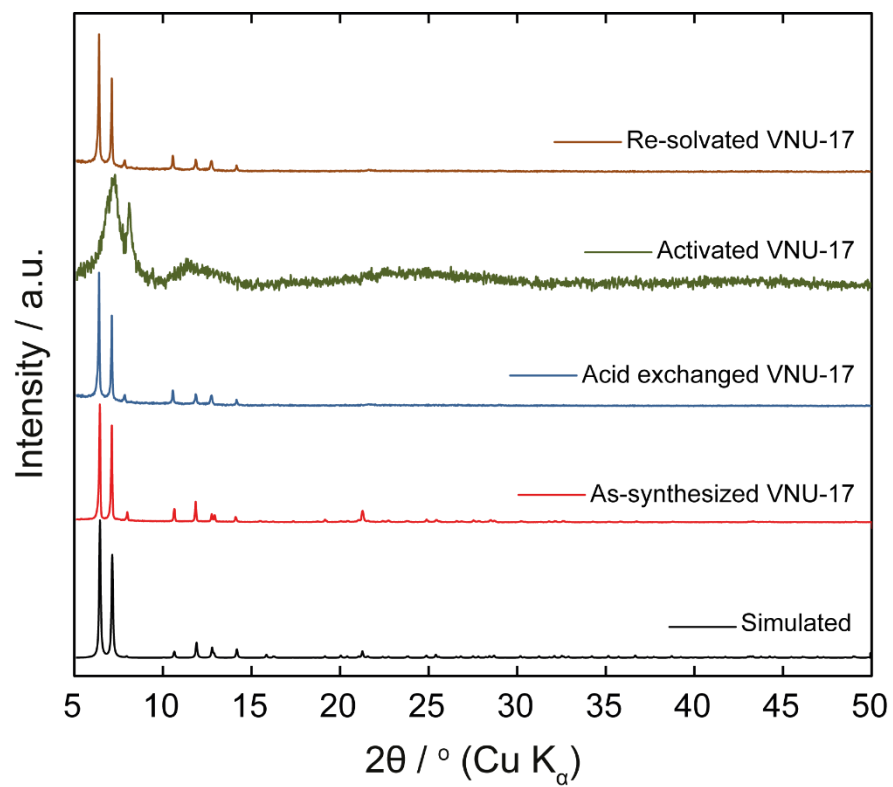


**Figure S3.** Powder X-ray diffraction patterns of VNU-17 after multistep-steps preparation.

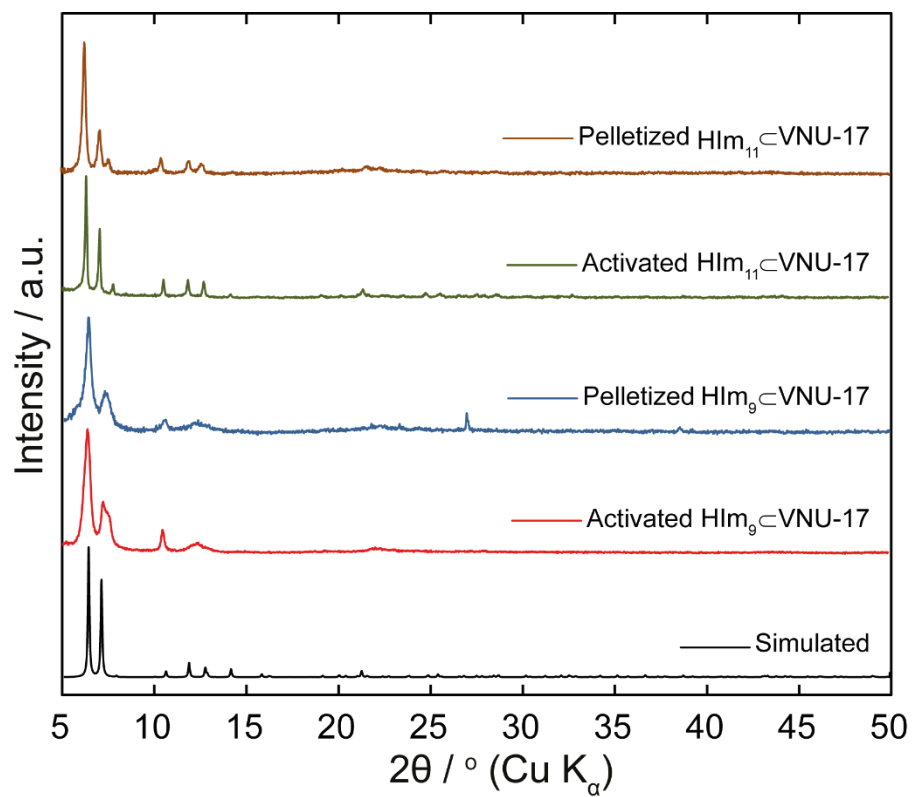


**Figure S4.** Powder X-ray diffraction patterns of  $\text{HIm}_9\text{cVNU-17}$ ,  $\text{HIm}_{11}\text{cVNU-17}$  and pelletized  $\text{HIm}_9\text{cVNU-17}$ ,  $\text{HIm}_{11}\text{cVNU-17}$  pressing at  $3.76 \text{ tons cm}^{-2}$ .

Section S6. Fourier Transform Infrared Analysis (FT-IR)

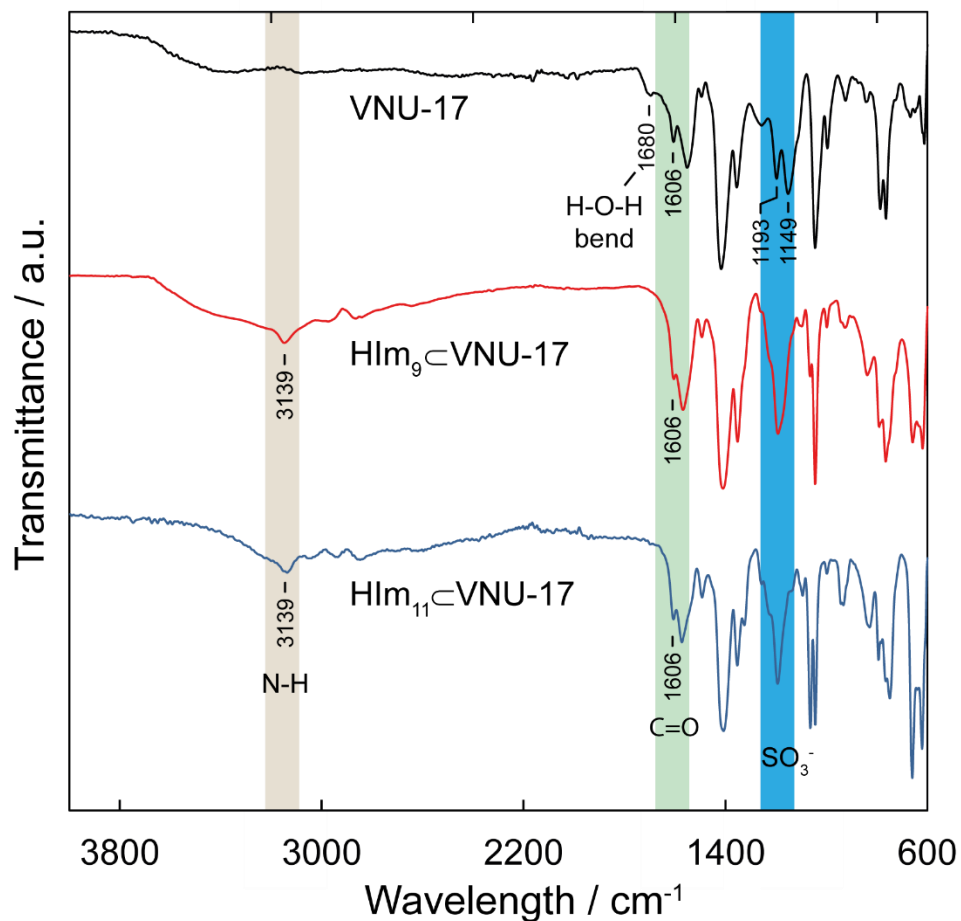


**Figure S5.** Fourier transform infrared analysis (FT-IR) of VNU-17, HIm<sub>9</sub>C-VNU-17 and HIm<sub>11</sub>C-VNU-17.

**Section S7. Thermal Gravimetric Analyses (TGA)**

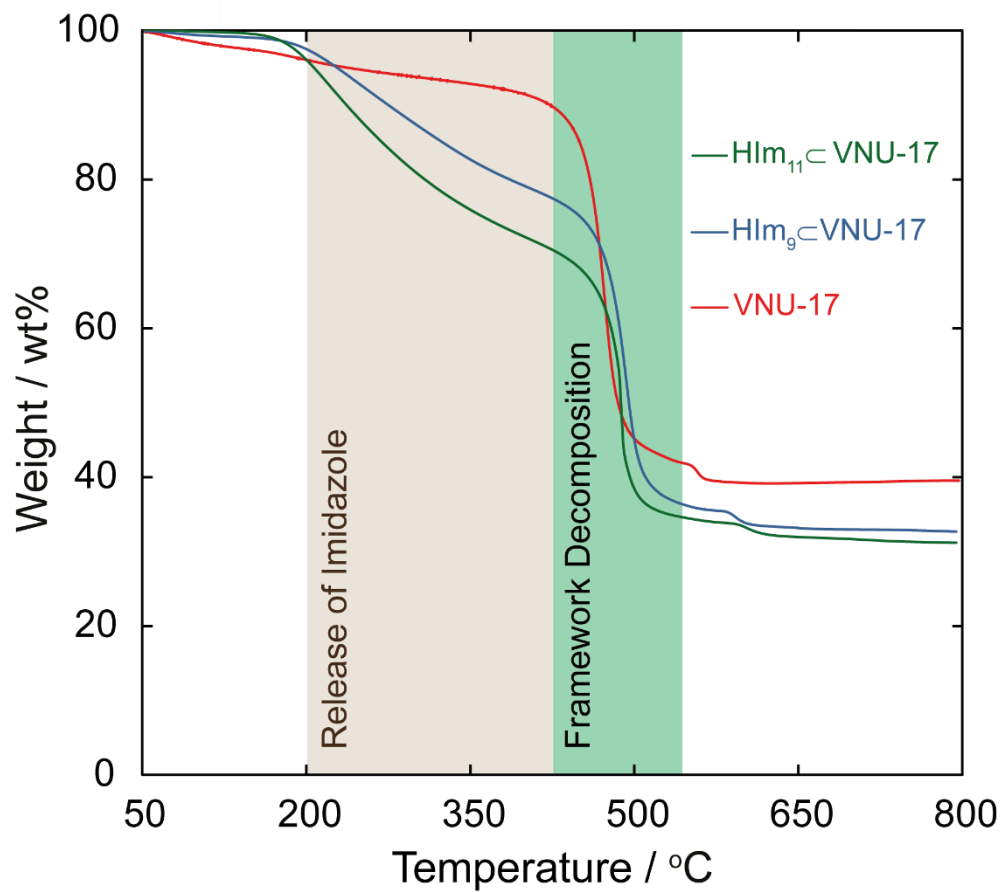


**Figure S6.** TGA analysis of VNU-17, HIm<sub>9</sub>C VNU-17 and HIm<sub>11</sub>C VNU-17.

**Section S8.** N<sub>2</sub> Adsorption Isotherm of VNU-17

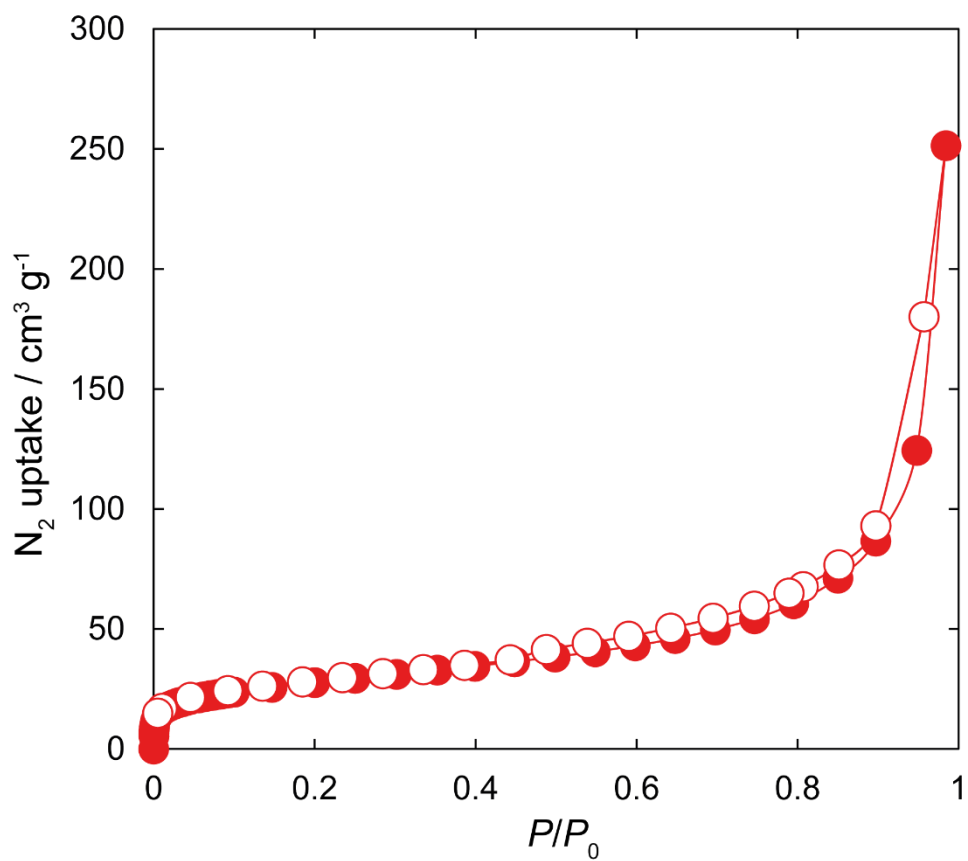


**Figure S7.** N<sub>2</sub> uptake of VNU-17 at 77 K. The closed and open circles represent the adsorption and desorption branches of the isotherm, respectively. The connecting line functions as a guide for the eye.

**Section S9.** Stability of VNU-17 in Water

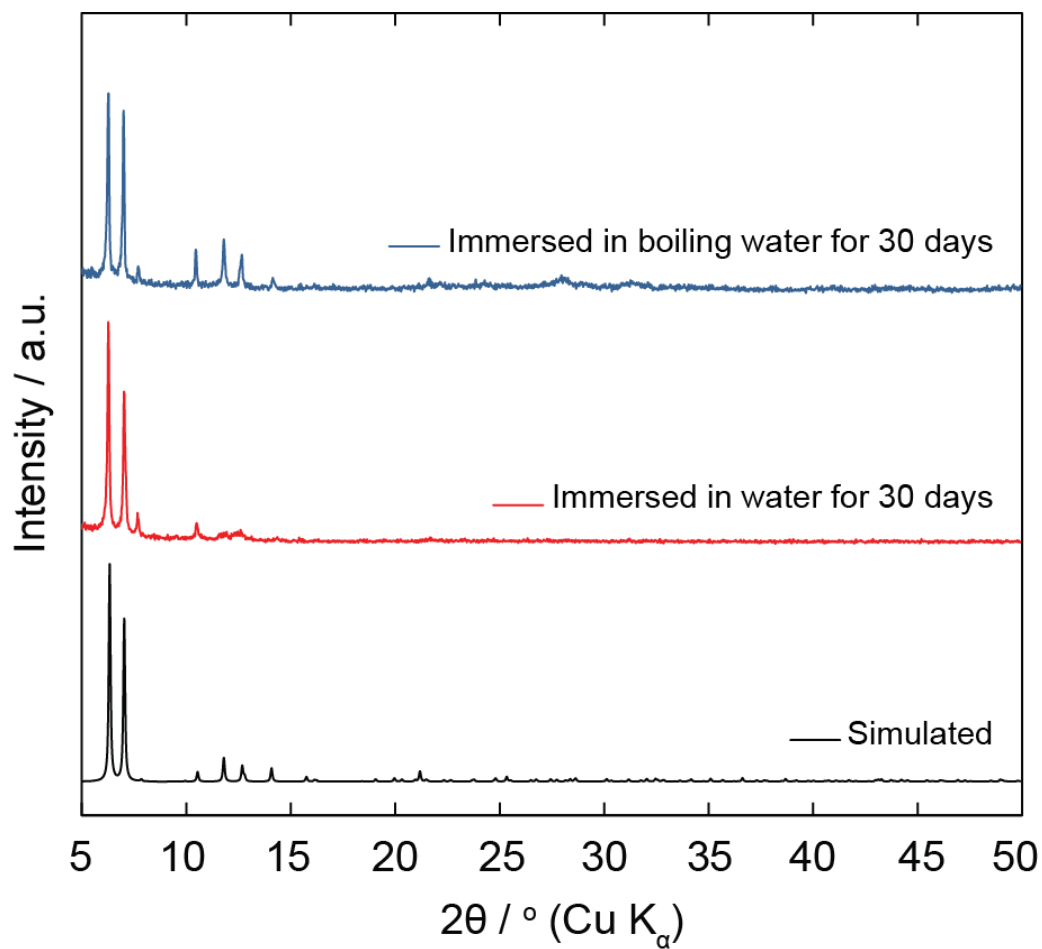


**Figure S8.** Powder X-Ray diffraction patterns of VNU-17 in water for 30 days

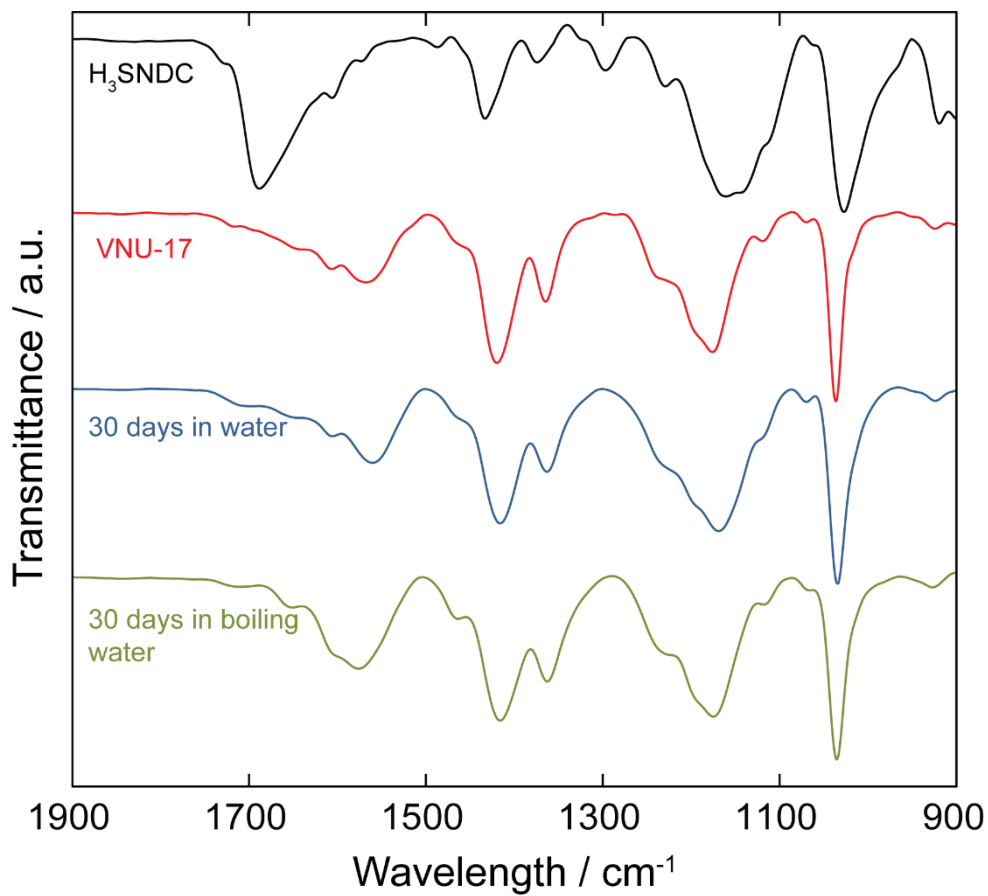


**Figure S9.** Fourier transform infrared analysis (FT-IR) of VNU-17 in water for 30 days

## Section S10. <sup>1</sup>H-NMR Analysis of Digested Samples

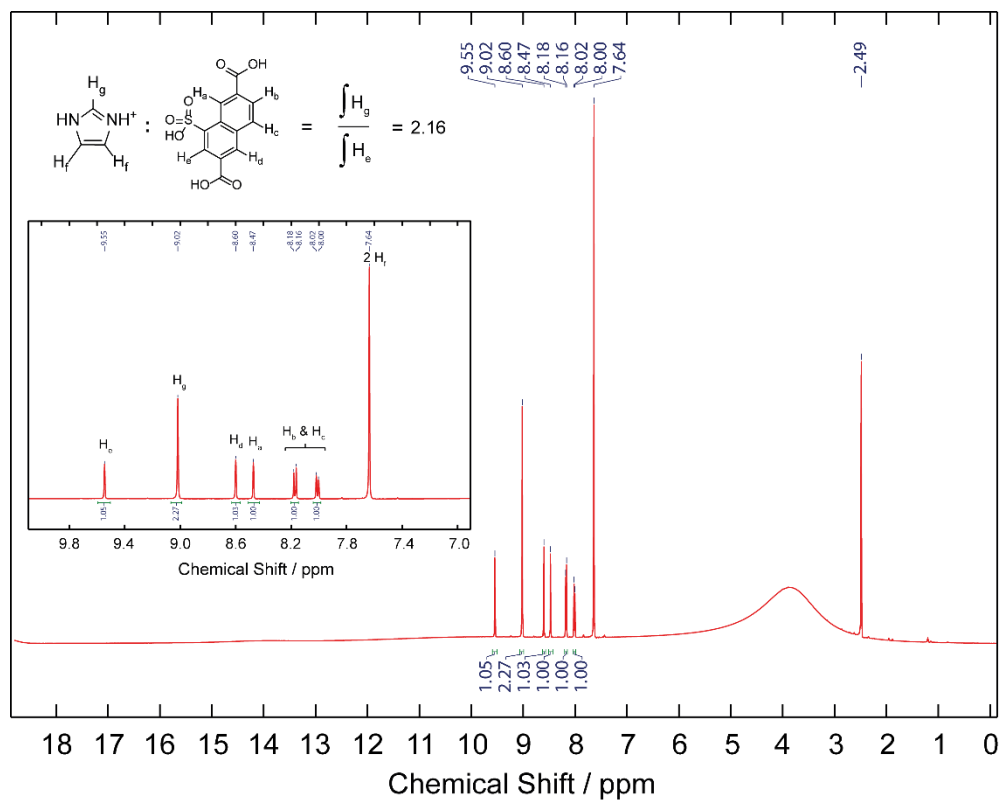


**Figure S10.** <sup>1</sup>H-NMR analysis of digested HIm<sub>9</sub>C-VNU-17

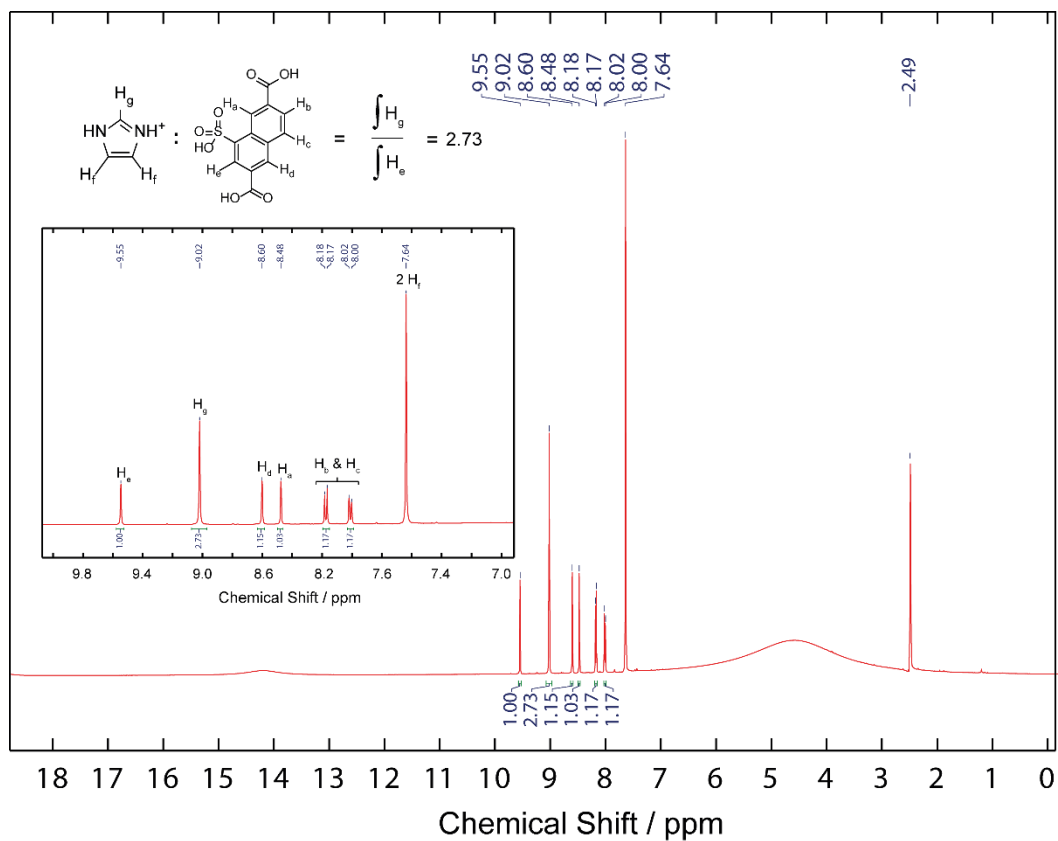


**Figure S11.** <sup>1</sup>H-NMR analysis of digested HIm<sub>11</sub>C-VNU-17.

Section S11. Rietveld Refinement of  $\text{HfM}_{11}\text{C-VNU-17}$

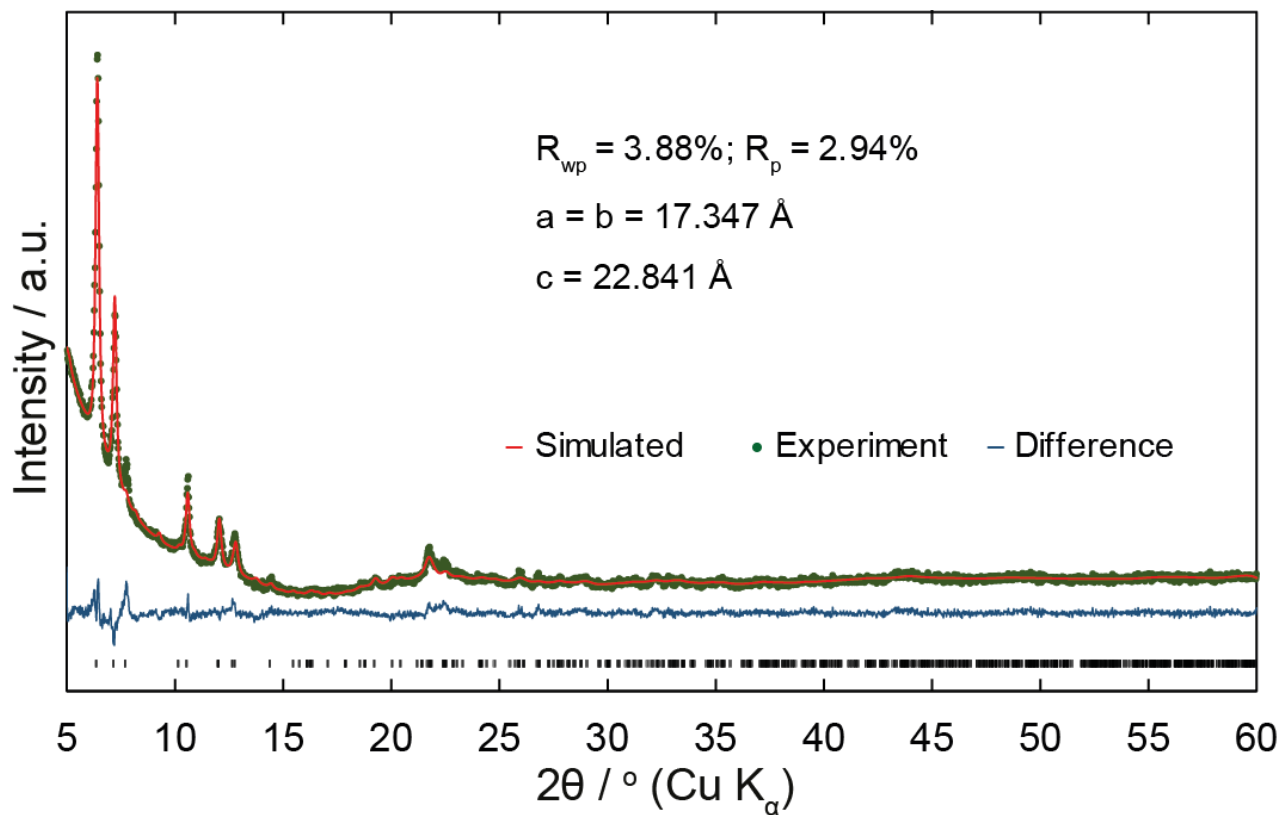


**Figure S12.** The Rietveld refinements using  $P_1$  space group of  $\text{HfM}_{11}\text{C-VNU-17}$ : The experimental (green), refined (red), and difference (blue) patterns. The Bragg positions are marked as black bars.

Section S12. Water Adsorption Studies

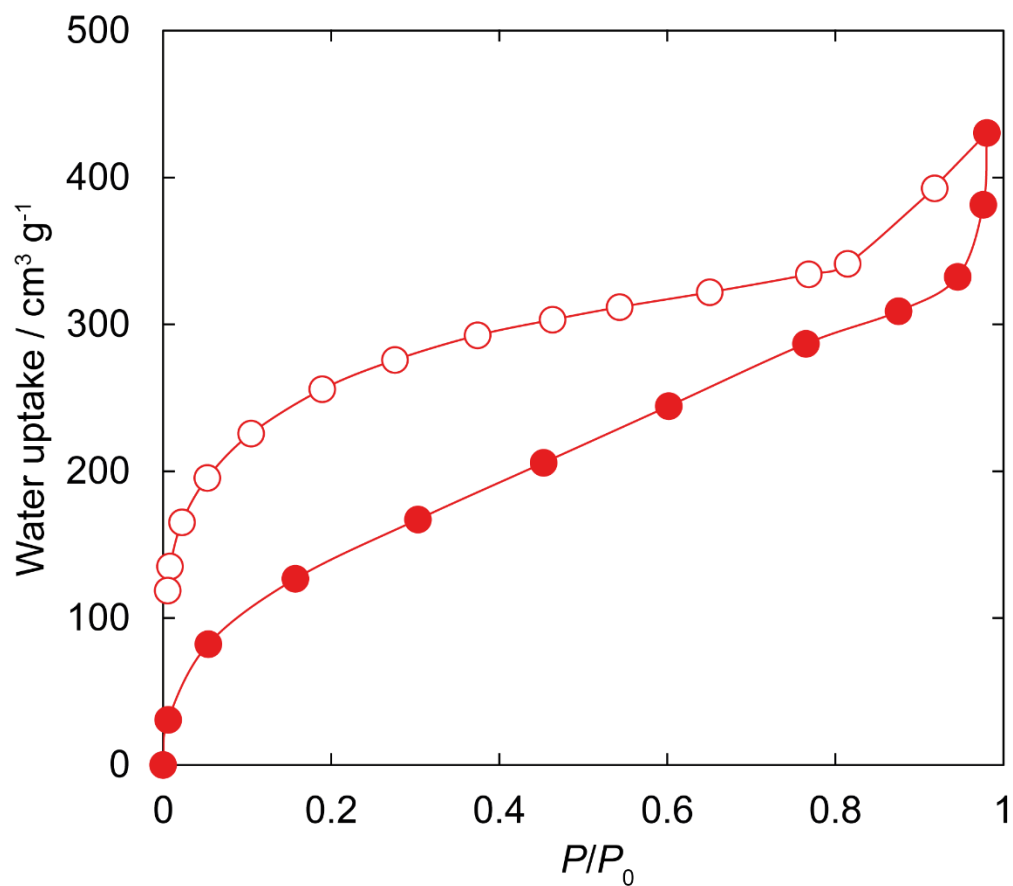
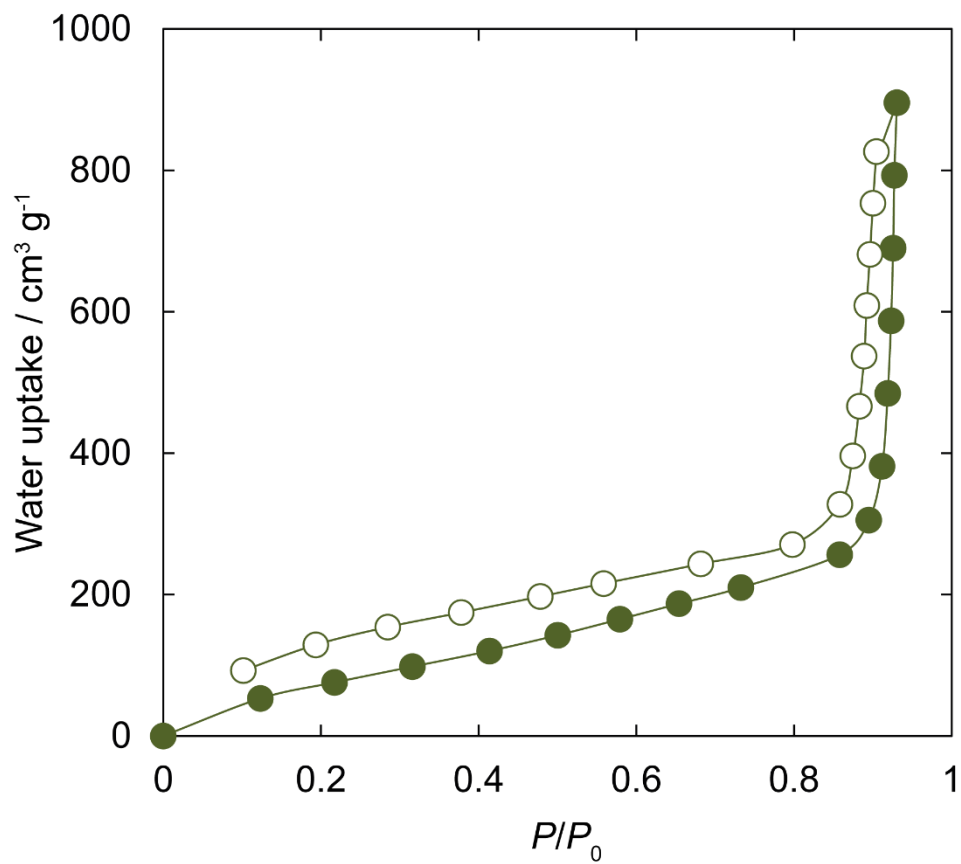
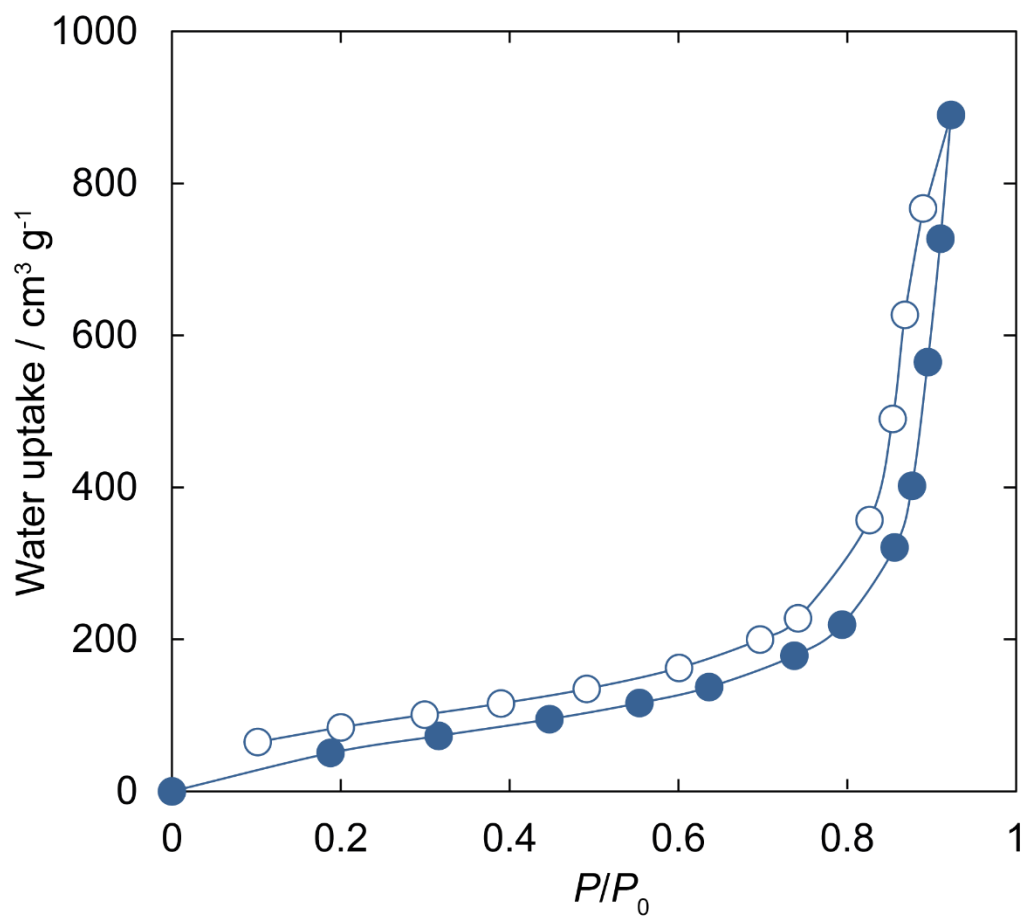


Figure S13. Water uptake of VNU-17 at 25 °C as a function of  $P/P_0$



**Figure S14.** Water uptake of Hlm<sub>9</sub>-VNU-17 at 25 °C as a function of  $P/P_0$



**Figure S15.** Water uptake of Hlm<sub>11</sub>C-VNU-17 at 25 °C as a function of  $PIP_0$

### Section S13. Proton Conductivity Studies

It is noted that the impedance of the electric wire without pelleted sample was collected in order to correct for the inductive effect. The correction was carried out by subtracting the experimental impedance of pelletized sample from the experimental impedance of the electric wire in order to obtain the pure impedance of pelletized sample.

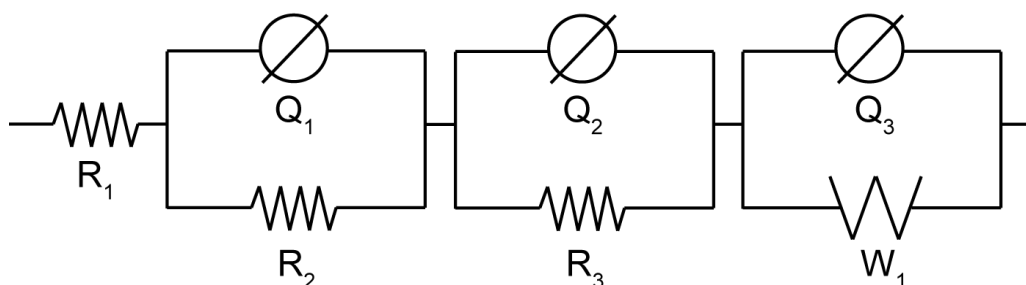


**Figure S16.** An equivalent circuit used for fitting. Schematic representations:  $W_1$ , Warburg diffusion element;  $Q_1/Q_2/Q_3$ , imperfect capacitor;  $R_1$ , Contact resistor;  $R_2$ , bulk resistor;  $R_3$ , grain boundary resistor.

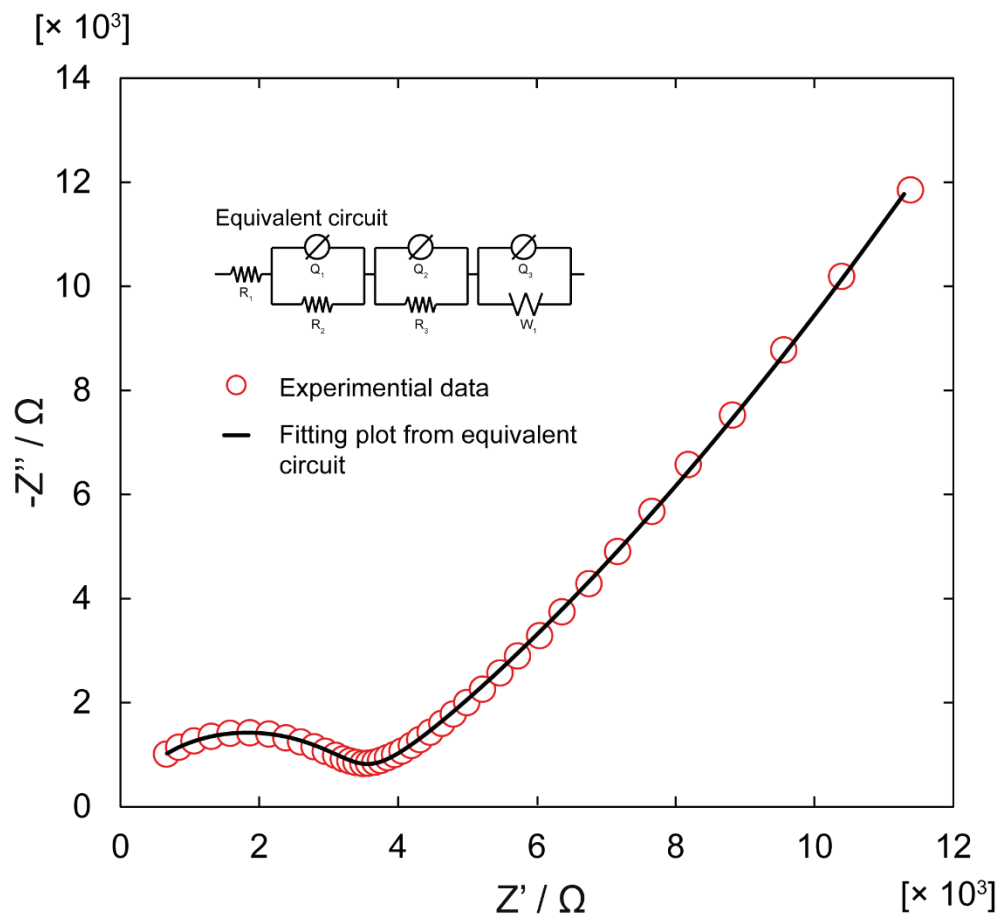


**Figure S17.** Nyquist plot derived from equivalent circuit (black line) and experimental Nyquist plot (red circles) of pelletized VNU-17 under 98% RH at 70 °C. Frequency ranged from 1 MHz to 10 Hz.

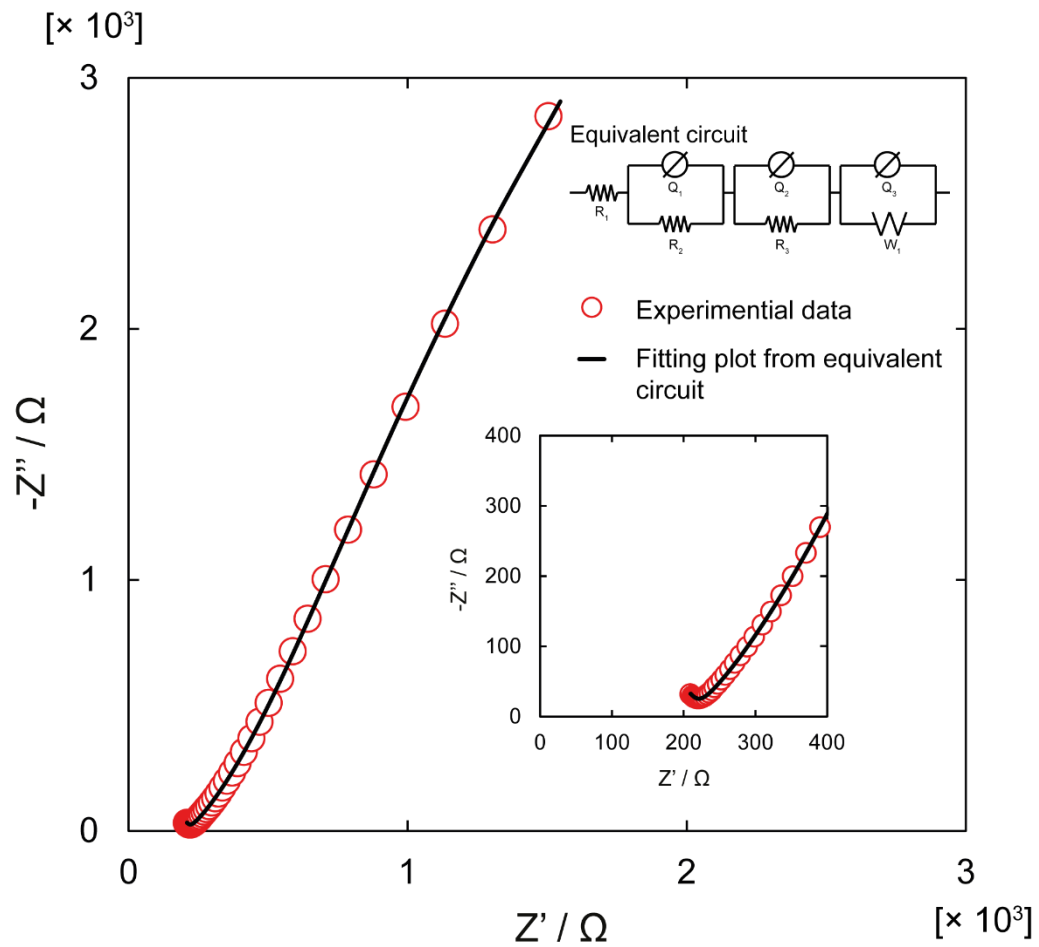


**Figure S18.** Nyquist plot derived from equivalent circuit (black line) and experimental Nyquist plot (red circles) of pelletized HIm<sub>9</sub>C/VNU-17 under 85% RH at 70 °C. Frequency ranged from 1 MHz to 10 Hz. Inset: Zoom of Nyquist plot at high frequency.

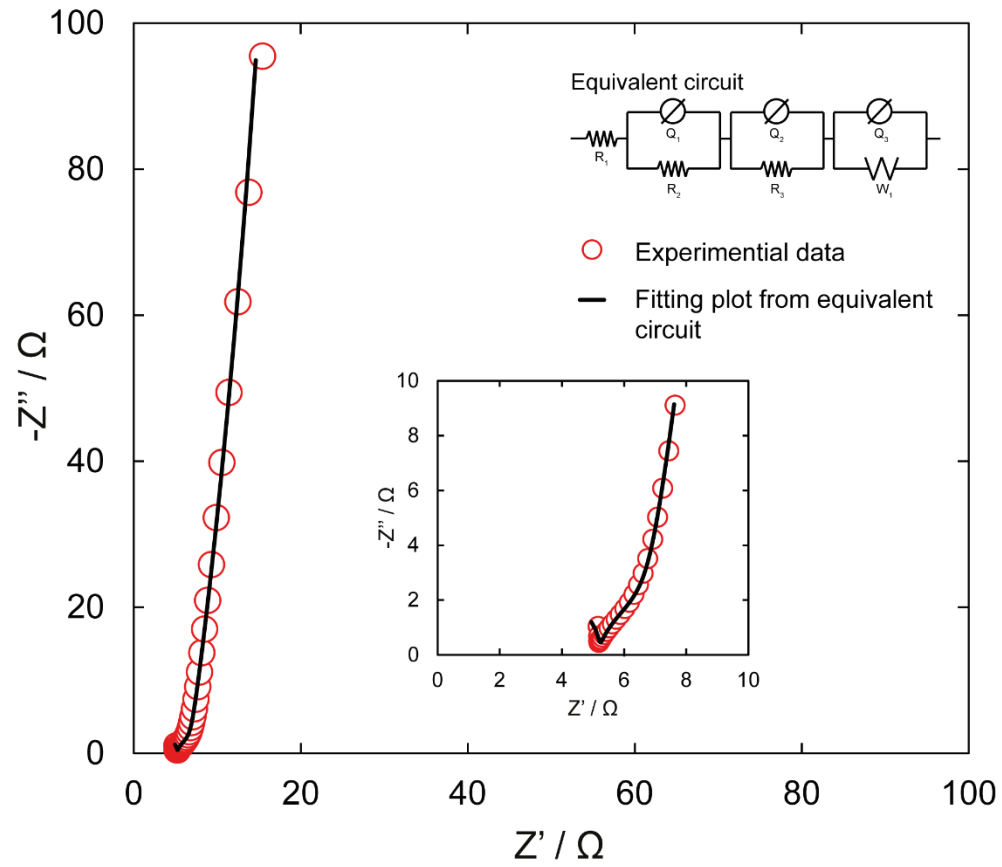


**Figure S19.** Nyquist plot derived from equivalent circuit (black line) and experimental Nyquist plot (red circles) of pelletized H1m11C-VNU-17 under 85% RH at 70 °C. Frequency ranged from 1 MHz to 10 Hz. Inset: Zoom of Nyquist plot at high frequency.

**Table S2.** Conductivity of VNU-17 under 98% RH from 30 °C to 70 °C.

Temperature / °C	$\sigma / \text{S cm}^{-1}$
30	$9.00 \times 10^{-7}$
40	$1.57 \times 10^{-6}$
50	$2.71 \times 10^{-6}$
60	$4.27 \times 10^{-6}$
70	$6.65 \times 10^{-6}$

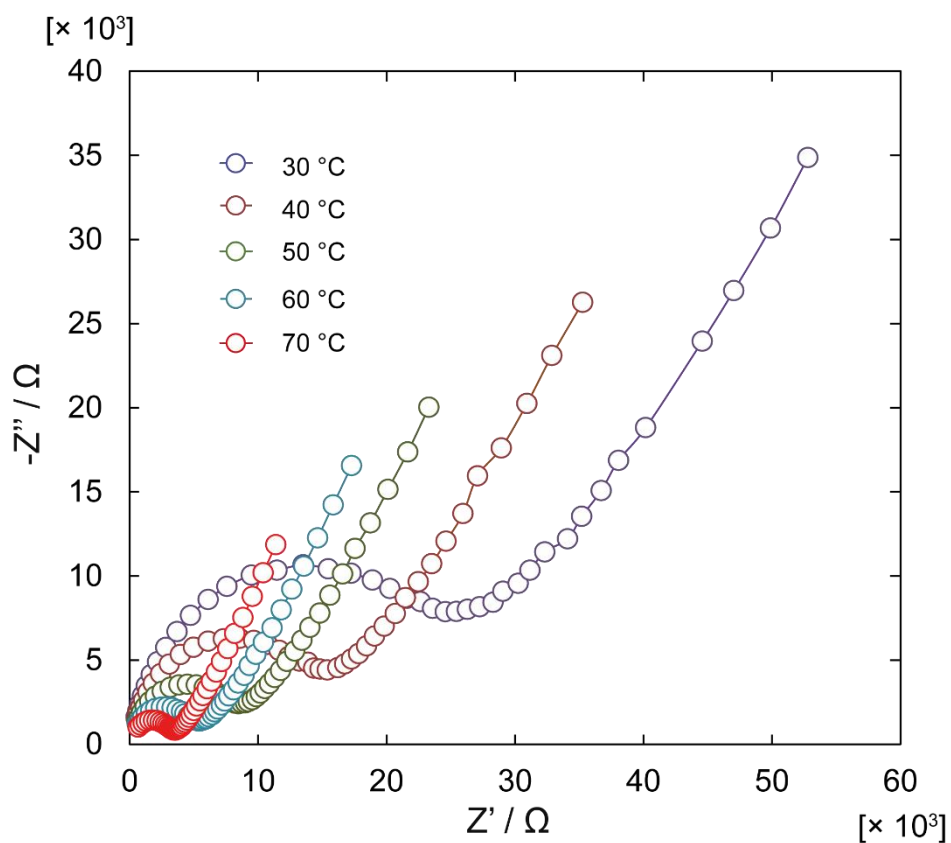


**Figure S20.** Nyquist plots of pelletized VNU-17 under 98% RH from 30 °C to 70 °C.

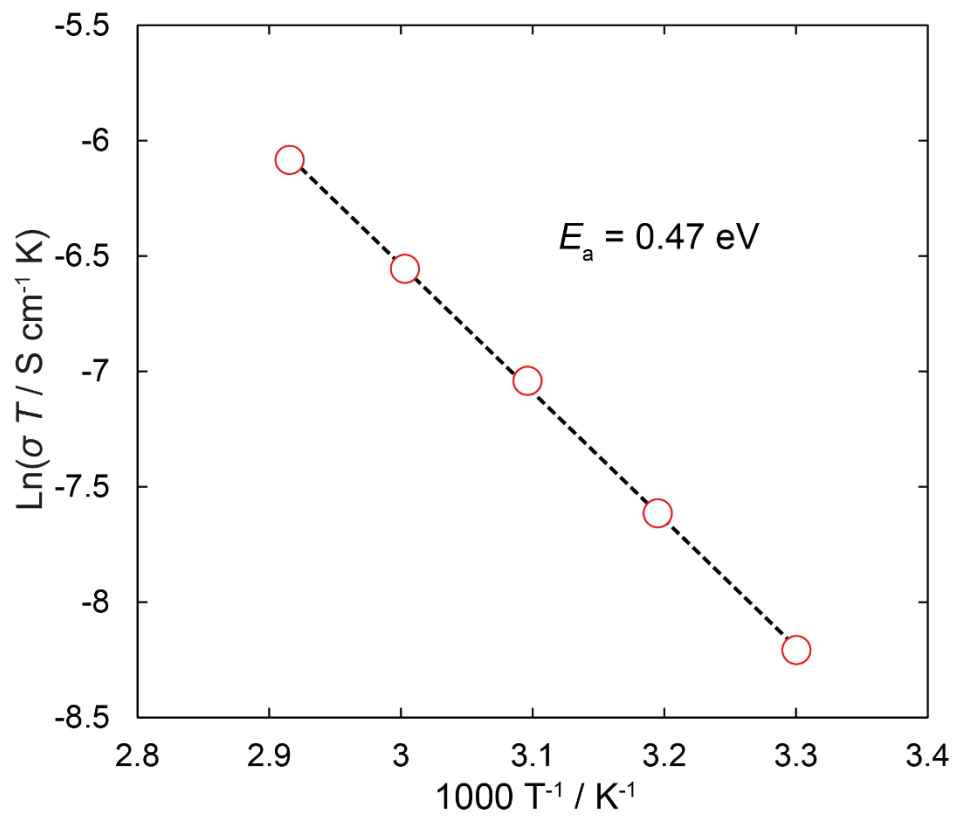


**Figure S21.** Arrhenius plot of VNU-17 at 98% RH.

**Table S3.** Conductivity of VNU-17 at 70 °C from 50% RH to 98% RH.

Relative Humidity / %	$\sigma / \text{S cm}^{-1}$
50	$3.02 \times 10^{-8}$
60	$7.05 \times 10^{-8}$
70	$1.50 \times 10^{-7}$
80	$3.26 \times 10^{-7}$
90	$7.63 \times 10^{-7}$
98	$6.65 \times 10^{-6}$

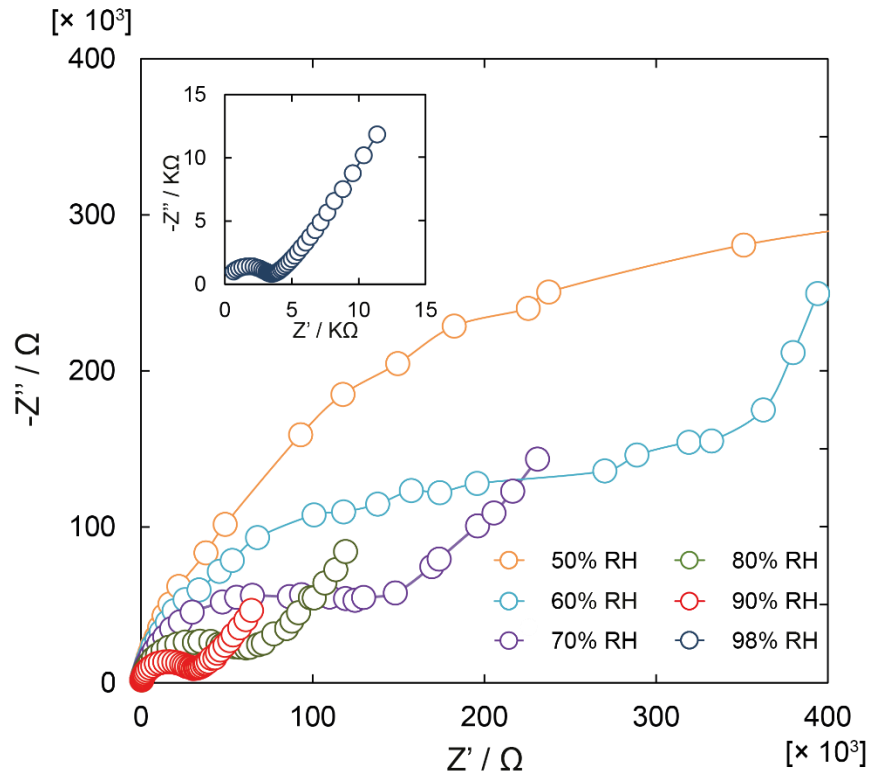


**Figure S22.** Nyquist plots of pelletized VNU-17 at 70 °C under relative humidity varied from 50% to 98%.

**Table S4.** Conductivity of HIm<sub>9</sub>C-VNU-17 under 85% RH from 30 °C to 70 °C.

Temperature / °C	$\sigma / \text{S cm}^{-1}$
30	$2.06 \times 10^{-5}$
40	$3.56 \times 10^{-5}$
50	$5.65 \times 10^{-5}$
60	$8.93 \times 10^{-5}$
70	$1.53 \times 10^{-4}$

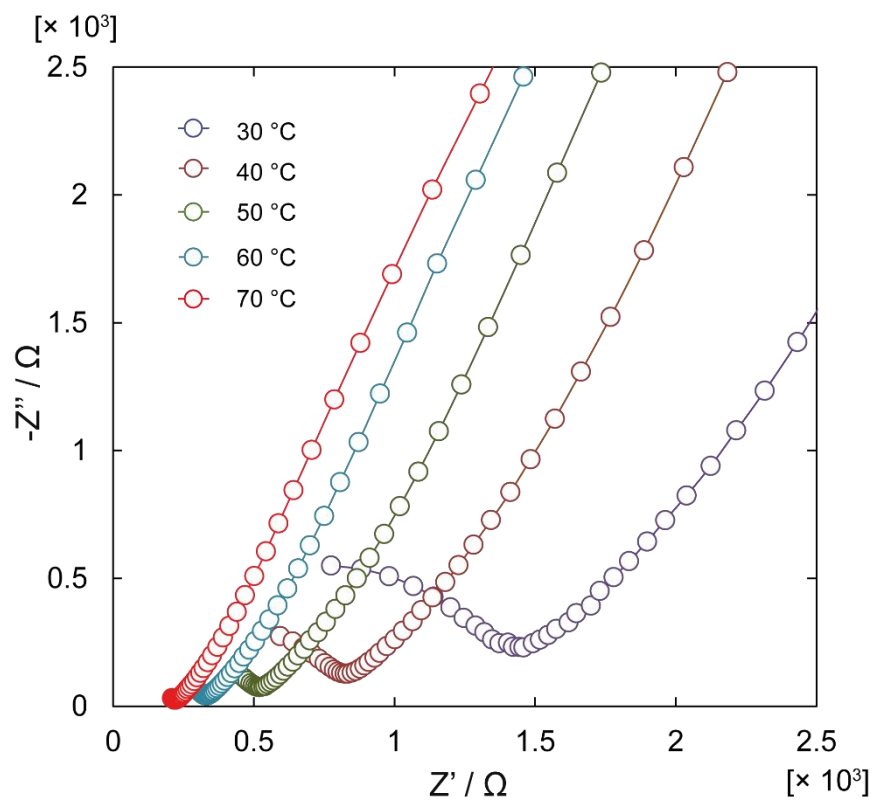


**Figure S23.** Nyquist plots of pelletized HIm<sub>9</sub>C-VNU-17 under 85% RH from 30 °C to 70 °C.

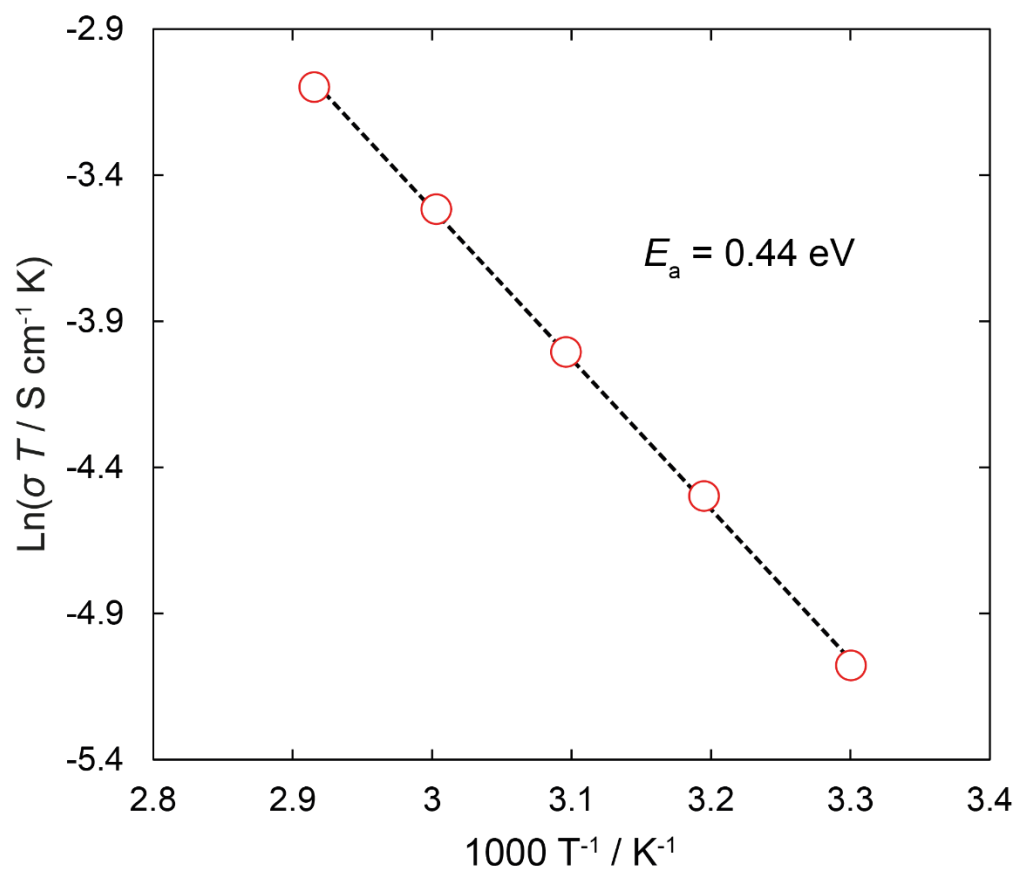


**Figure S24.** Arrhenius plot of HIm<sub>9</sub>C-VNU-17 at 85% RH.

**Table S5.** Conductivity of Hlm<sub>9</sub>-VNU-17 at 70 °C from 50% RH to 85% RH.

Relative Humidity / %	$\sigma / \text{S cm}^{-1}$
50	$1.22 \times 10^{-5}$
60	$2.40 \times 10^{-5}$
70	$5.33 \times 10^{-5}$
80	$9.89 \times 10^{-5}$
85	$1.53 \times 10^{-4}$

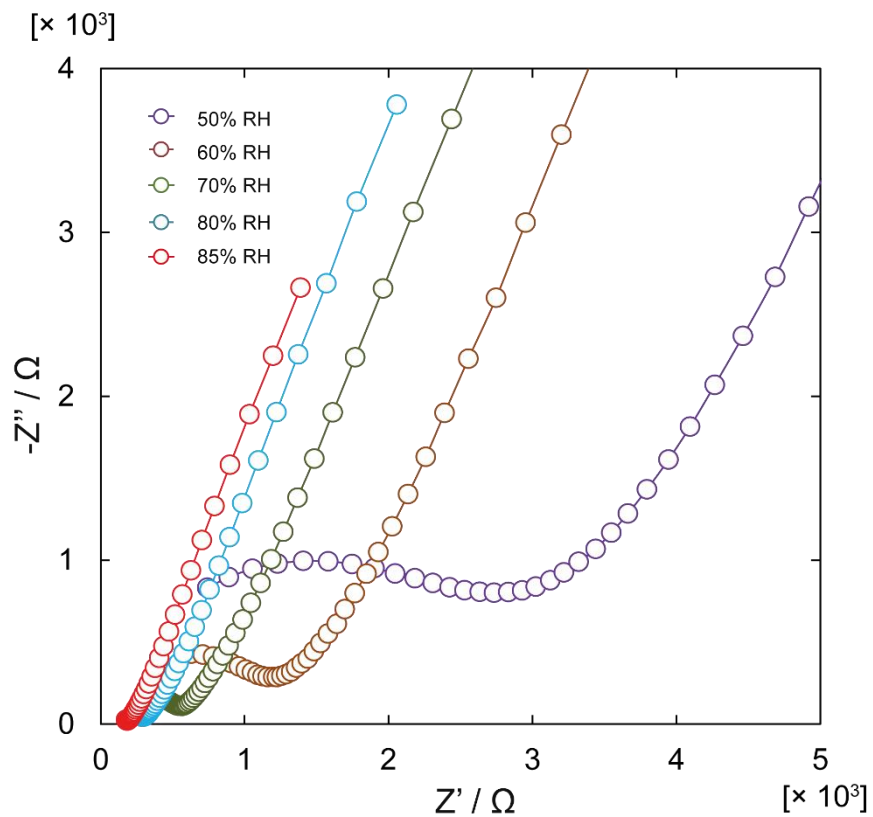


**Figure S25.** Nyquist plots of pelletized Hlm<sub>9</sub>-VNU-17 at 70 °C under relative humidity varied from 50% to 85%.

**Table S6.** Conductivity of Hlm<sub>11</sub>⊂VNU-17 under 85% RH from 30 °C to 70 °C.

Temperature / °C	$\sigma / \text{S cm}^{-1}$
30	$2.00 \times 10^{-3}$
40	$2.90 \times 10^{-3}$
50	$3.94 \times 10^{-3}$
60	$4.94 \times 10^{-3}$
70	$5.93 \times 10^{-3}$

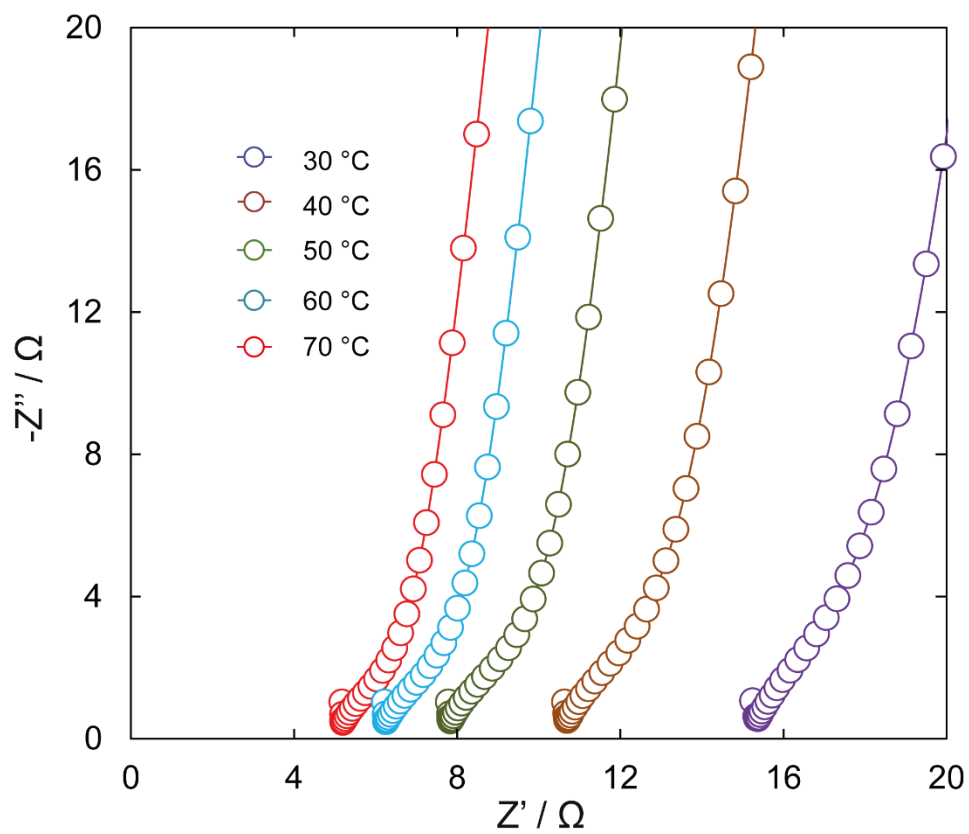


**Figure S26.** Nyquist plots of pelletized Hlm<sub>11</sub>⊂VNU-17 under 85% RH from 30 °C to 70 °C.

**Table S7.** Conductivity of Hlm<sub>11</sub>C-VNU-17 at 70 °C from 50% RH to 85% RH.

Relative Humidity / %	$\sigma / \text{S cm}^{-1}$
50	$3.32 \times 10^{-4}$
60	$6.53 \times 10^{-4}$
70	$1.04 \times 10^{-3}$
80	$3.72 \times 10^{-3}$
85	$5.93 \times 10^{-3}$

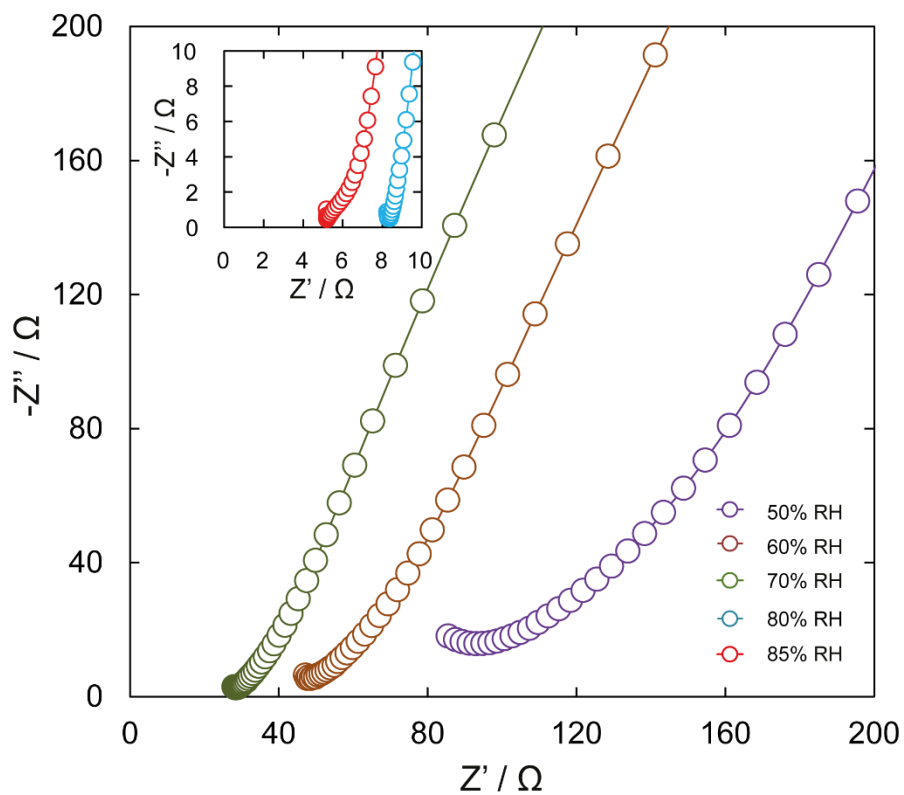


**Figure S27.** Nyquist plots of pelletized Hlm<sub>11</sub>C-VNU-17 at 70 °C under relative humidity ranged from 50% to 85%.

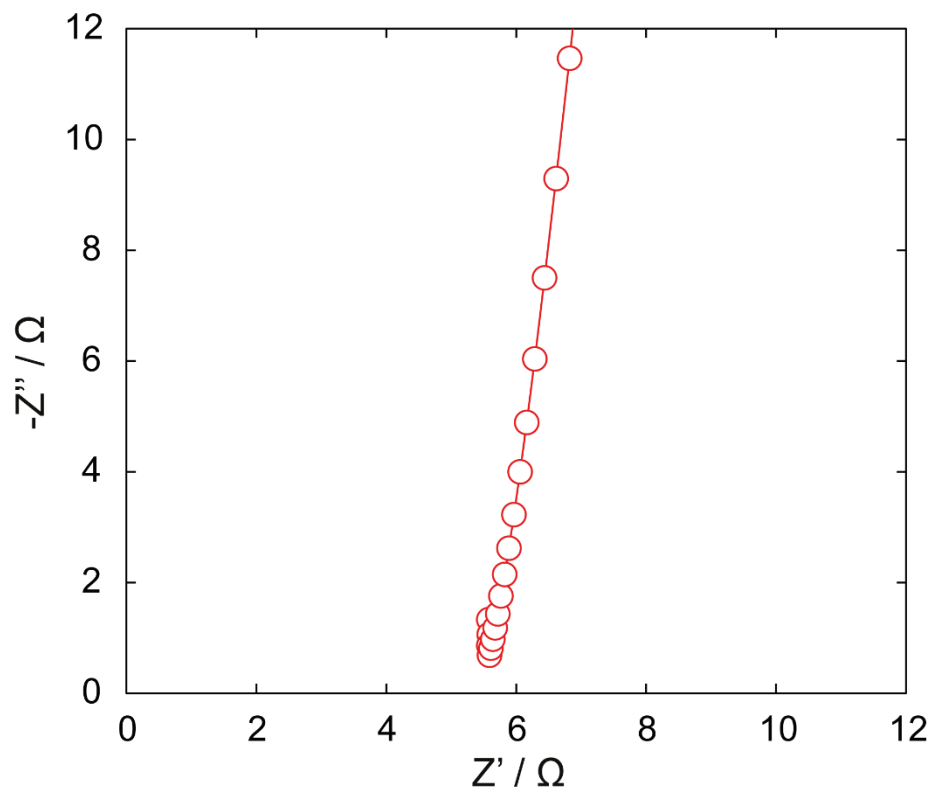


**Figure S28.** Nyquist plot of pelletized HIm<sub>11</sub>C/VNU-17 at 85% RH at 70 °C after 40 h of consecutive ac impedance measurements.

**Section S14.** Stability of HIm<sub>11</sub>⊂VNU-17 during Proton Conductivity Studies

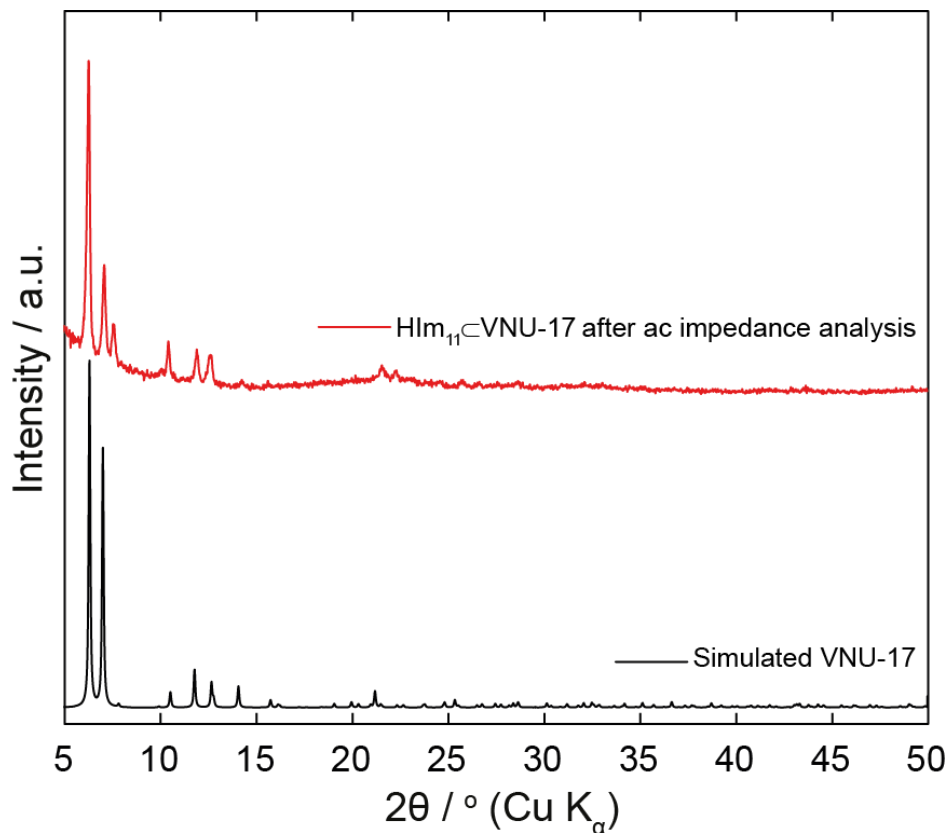


**Figure S29.** Simulated PXRD pattern of VNU-17 (black) as compared to the experimental pattern from the subjecting pelletized HIm<sub>11</sub>⊂VNU-17 to time-dependent ac impedance measurements at 85% RH and 70 °C for 40 hours (red).

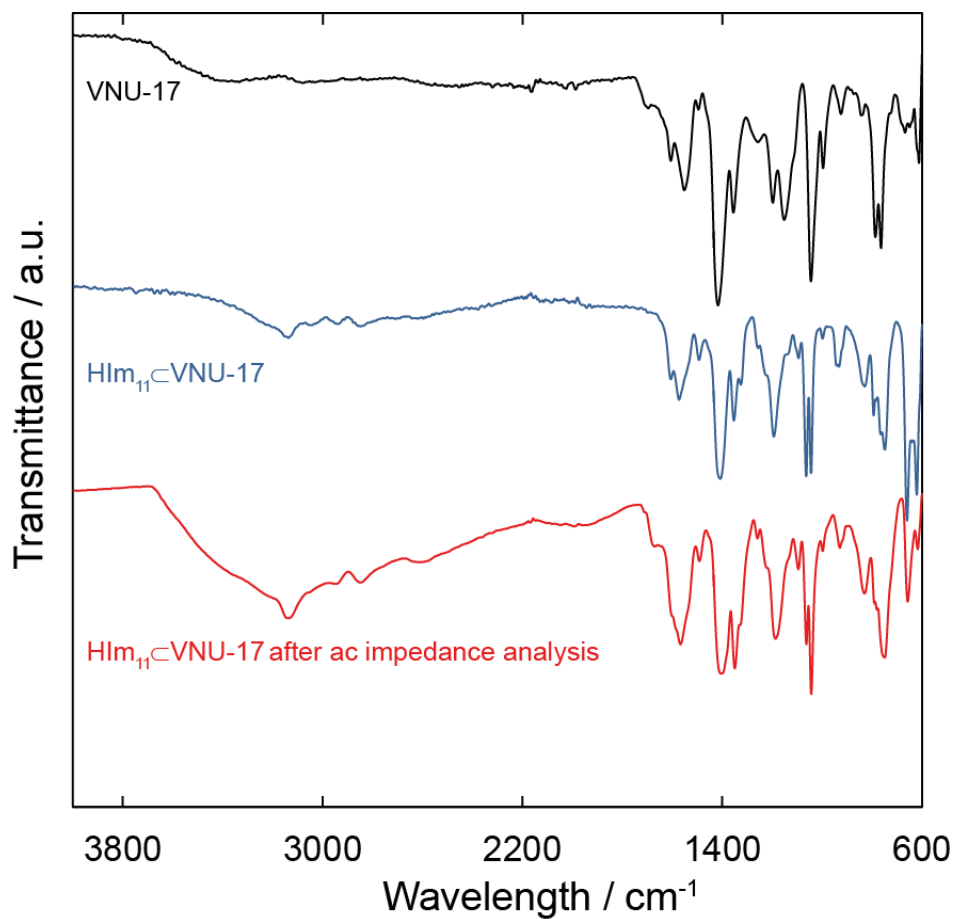


**Figure S30.** FT-IR spectra of VNU-17 (black) as compared to the FT-IR spectra from HIm<sub>11</sub>@VNU-17 (blue) and the subjecting pelletized HIm<sub>11</sub>@VNU-17 to time-dependent ac impedance measurements at 85% RH and 70 °C for 40 hours (red).